Inhibition of Bacteriophage T7 RNA Polymerase *in Vitro* Transcription by DNA-Binding Pyrrolo[2,1-*c*][1,4]benzodiazepines†

Madhu S. Puvvada,‡ Stephen A. Forrow,§ John A. Hartley,§ Pauline Stephenson,|| Ian Gibson,|| Terence C. Jenkins,⊥ and David E. Thurston*,‡

Gene Targeted Drug Design Research Group, School of Pharmacy and Biomedical Science, University of Portsmouth, Portsmouth PO1 2DT, U.K., CRC Drug DNA Interactions Research Group, Department of Oncology, University College London Medical School, London W1P 8BT, U.K., School of Biological Sciences, University of East Anglia, Norwich NR4 7JT, U.K., and CRC Biomolecular Structure Unit, The Institute of Cancer Research, Sutton, Surrey SM2 5NG, U.K.

Received October 19, 1995; Revised Manuscript Received October 28, 1996⊗

ABSTRACT: The interactions of several pyrrolo[2,1-*c*][1,4]benzodiazepine (PBD) antitumor antibiotics with linearized plasmid pGEM-2-N-*ras* DNA have been analyzed by quantitative *in vitro* transcription (QIVT) and *in vitro* transcription footprinting (IVTF) methods. A concentration-dependent inhibitory effect of the PBDs on transcription is observed using both techniques. The rank order for overall inhibition of transcription by the QIVT method is found to be: sibiromycin > tomaymycin > anthramycin > DC-81 > neothramycin, whereas the IVTF experiments show a different ranking: sibiromycin > anthramycin > neothramycin > tomaymycin. In addition, stimulation of transcription was observed at low PBD concentrations in both the QIVT and IVTF experiments. These results demonstrate unequivocally that the formation of PBD−DNA adducts at A**G**A-5′ base sequences on the transcribed strand results in transcription blockage for all PBDs examined. Furthermore, the sequence of flanking base pairs appears to influence the degree of blocking, with the sequences ACA**G**AAA-5′, AAA**G**ATG-5′, AGA**G**ATA-5′, and CAA**G**AAC-5′ providing the most pronounced blocks for all PBDs studied in this system. Neothramycin and tomaymycin cause additional blocks at some G**G**A-5′ and T**G**A-5′ sequences. Parallel MPE−Fe(II) footprinting studies have revealed PBD binding sites on both the transcribing and nontranscribing strands, although all transcription blocks determined from the IVTF assays are due to drug bound on the transcribing DNA template strand.

Pyrrolo[2,1-*c*][1,4]benzodiazepines (PBDs;[1] Figure 1) are a class of sequence-selective DNA-binding antitumor antibiotics that form covalent adducts (Figure 2) with the exocyclic N2 of guanine in the minor groove of double-stranded DNA (Remers, 1988; Thurston, 1993). These agents are characterized by an (*S*)-configuration at the B−C ring junction which causes a right-handed envelope-type molecular twist when viewed from the aromatic A-ring toward the C-ring. This feature provides the appropriate three-dimensional shape for isohelical interaction with the minor groove of B-form DNA, leading to a snug fit at the binding site. Well-known members of the PBD family include tomaymycin, anthramycin, sibiromycin, DC-81, and neothramycin (Figure 1).

Previous footprinting-type studies have shown that the adducts span 3 base pairs with a rank order of preference for 5′-Pu-**G**-Pu > 5′-Pu-**G**-Py or 5′-Py-**G**-Pu > 5′-Py-**G**-Py sequences (Hertzberg et al., 1986; Hurley et al., 1988; Thurston, 1993). Recent high-field NMR, crystallographic, and molecular modeling studies have provided detailed information about the precise three-dimensional structure of DNA−PBD adducts, including orientation of the molecule within the host minor groove and stereochemistry at the C11 position (Kopka et al., 1994; for a review, see: Thurston, 1993). Thermal denaturation (ΔT_m), ethidium bromide displacement (EB_{60}), and restriction endonuclease digestion (RED_{100}) studies have shown that the rank order of DNA reactivity for the naturally-occurring PBDs is sibiromycin > anthramycin > tomaymycin > DC-81 > neothramycin (Puvvada et al., 1993). However, there is little understanding of the relationship between DNA-binding affinity, sequence selectivity, and either *in vitro* cytotoxicity or *in vivo* antitumor activity.

The aim of this study was to investigate the effects of five PBDs (Figure 1) of differing inherent reactivity upon *in vitro* transcription, and to identify the DNA sequences that may be responsible for blockage of transcription. Two methods were employed: (i) a quantitative *in vitro* transcription assay (QIVT) using TCA precipitation, which involves monitoring the effect of a PBD upon inhibition of T7 RNA polymerase

† This work was supported by the Cancer Research Campaign of the U.K. (SP1938/0301 to D.E.T.).

* Address correspondence to: Professor David E. Thurston, Director, CRC Gene Targeted Drug Design Research Group, School of Pharmacy and Biomedical Science, University of Portsmouth, St. Michael's Building, White Swan Rd., Portsmouth, Hants. PO1 2DT, U.K. Phone: (+44) 01705-843598 (Direct); Mobile: (+44) 0973-499429; Fax: (+44) 01705-843573; E-Mail: david.thurston@port.ac.uk.

‡ University of Portsmouth.

§ University College London Medical School.

|| University of East Anglia.

⊥ The Institute of Cancer Research, Sutton.

⊗ Abstract published in *Advance ACS Abstracts,* February 1, 1997.

[1] Abbreviations: DTT, dithiothreitol; EB_{60}, ethidium bromide displacement assay; EDTA, ethylenediaminetetraacetic acid; IVTF, *in vitro* transcription footprinting assay; MPE−Fe(II), methidiumpropyl-EDTA−Fe(II); PBD, pyrrolo[2,1-*c*][1,4]benzodiazepine; QIVT, quantitative *in vitro* transcription assay; RED_{100}, restriction endonuclease digestion assay; TBE, Tris/boric acid/EDTA buffer; TCA, trichloroacetic acid; T_m, thermal denaturation.

S0006-2960(95)02490-1 CCC: $14.00

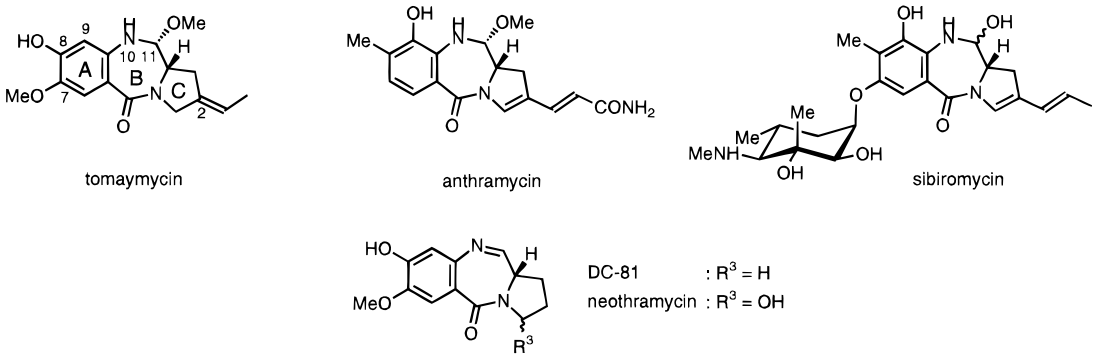

FIGURE 1: Structures of the pyrrolo[2,1-*c*][1,4]benzodiazepine (PBD) compounds used in this study, showing the ring numbering scheme.

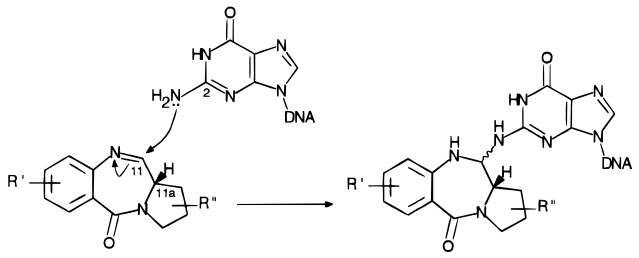

FIGURE 2: Proposed mechanism for covalent reaction with DNA, showing formation of an aminal bond between the C11 position of the PBD and the exocyclic N2 of a guanine base.

transcription, and (ii) an *in vitro* transcription footprinting (IVTF) technique established by Phillips and co-workers (Phillips & Crothers, 1986; Skorobogaty et al., 1988; White & Phillips, 1988, 1989a−c; Phillips et al., 1989, 1990a−c, 1994; Trist & Phillips, 1989; Gray et al., 1991; Cullinane et al., 1994; Masta et al., 1994; Panousis & Phillips, 1994). The IVTF method involves the formation of a stable ternary complex consisting of a DNA template (pGEM-2-N-*ras*; pGEM with T7 promoter and 300-bp N-*ras*), T7 RNA polymerase, and a nascent labeled 14-mer RNA fragment. Following exposure to the PBD, this stable complex was elongated and the blockage of transcription resulted in RNA fragments of various lengths that relate directly to the PBD binding sites.

In addition, MPE−Fe(II) footprinting (Hertzberg et al., 1986) was carried out on the same DNA fragment in order to enable comparison of the footprint sites with the blockages observed in the *in vitro* transcription experiments.

MATERIALS AND METHODS

Materials. Anthramycin and tomaymycin methyl ethers, neothramycin (as a mixture of isomeric 3-*O*-butyl ethers), and sibiromycin were gifts from Hoffmann-La Roche Corp. (New Jersey, U.S.A.), Fujisawa Corp. (Ibaraki, Japan), the Institute of Microbial Chemistry (Tokyo, Japan), and Kyowa Hakko Kogyo Co. Ltd (Tokyo, Japan), respectively. DC-81 was synthesized in this laboratory (Bose et al., 1992; Bose & Thurston, 1993). Stock solutions of each PBD (1 mM) were prepared by dissolving the compounds in the minimum amount of methanol (Aldrich, HPLC grade) before making up to volume with sterile water. All solutions were stored at 4 °C.

Ultrapure nucleotide triphosphates (rGTP, rATP, rCTP, and rUTP) were purchased from Pharmacia. Bacteriophage T7 RNA polymerase, ribonuclease inhibitor (rRNasin), dithiothreitol (DTT), and bovine serum albumin (BSA; RNase/DNase-free) were purchased from Promega. 3′-Deoxyribonucleotides drGTP, drATP, drCTP, and drUTP were purchased from Boehringer Mannheim. Bacterial alkaline phosphatase, polynucleotide kinase, and *Hin*dIII and *Eco*RI restriction enzymes were purchased from BRL and used as supplied. Methidiumpropyl-EDTA (MPE, Dervan's reagent) was a gift from Prof. P. Dervan (UCLA, U.S.A). All chemicals and reagents were purchased from BRL and were of molecular biology grade. Radionucleotides [α-^{32}P]-UTP (800 Ci/mmol and 10 mCi/mL), [α-^{32}P]ATP (3000 Ci/mmol and 10 mCi/mL), and [γ-^{32}P]ATP (3000 Ci/mmol and 10 mCi/mL) were obtained from Amersham plc (U.K.). Whatman GF/A glass filter discs and Ecoscint scintillation fluid were purchased from Sigma and National Diagnostics, respectively.

DNA Source. A 334-bp N-*ras* fragment was ligated into the *Bam*HI site of pGEM-2. The resulting plasmid, denoted pGEM-2-N-*ras*, was transformed into *Escherichia coli* JM101 by using the calcium chloride procedure, then isolated and purified as described previously (Maniatis, 1989). The plasmid was subsequently linearized by digestion with *Eco*RI to produce a full-length transcript of 390 bases. The concentration and integrity of the DNA were determined by spectrophotometry using a molar extinction coefficient at 260 nm of 6600 M^{-1} cm^{-1}.

Quantitative in Vitro Transcription (QIVT) Assay. The linearized pGEM-2-N-*ras* was equilibrated in transcription (Tc) buffer (40 mM Tris-HCl, pH 7.5, 6 mM $MgCl_2$, 2 mM spermidine, and 10 mM DTT) containing 1 unit/μL RNase inhibitor, 2.5 mM each of the four rNTPs, and [α-^{32}P]UTP. The PBD was added at different PBD:DNA concentration ratios prior to addition of T7 RNA polymerase (20 units), and the final reaction mixture (20 μL) was incubated at 37 °C for 1 h in order to observe any concentration-dependent response. Reactions were stopped by the addition of 10 mM EDTA.

The percentage incorporation of the radiolabeled rUTP was determined by TCA precipitation. A 10-μL aliquot of each reaction mixture was spotted on a Whatman GF/A glass filter disc, dried, and counted using a Beckman LS1800 scintillation counter. The remaining reaction mixture was treated with ice-cold TCA solution [0.5 mL of 5% (w/v) trichloroacetic acid] and carrier nucleic acid tRNA, and the precipitate was captured on pre-wetted (1 mL of 5% TCA) Whatman GF/A glass filter discs held in a 12-position vacuum manifold (Millipore). The filters were washed free of unincorporated rUTP radiolabel with 10 mL of 5% TCA, followed by 10 mL of absolute ethanol, and then air-dried and placed in vials containing 5 mL of scintillation fluid; and the activity (cpm) was counted. The total counts and TCA precipitate counts

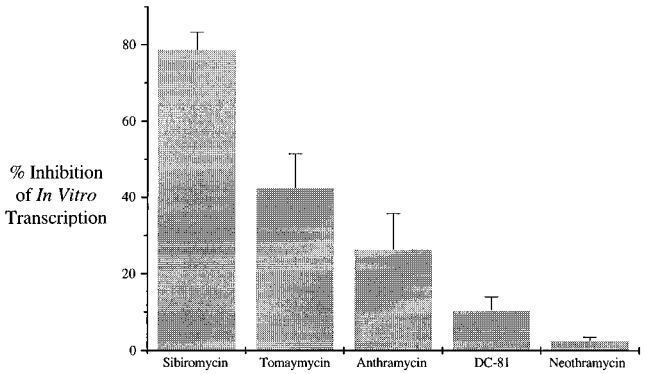

FIGURE 3: Inhibition of *in vitro* transcription by the PBD compounds at a concentration of 100 μM using the QIVT procedure. Each inhibitory activity was determined from the extent of incorporation of radiolabeled rUTP following TCA precipitation (see text).

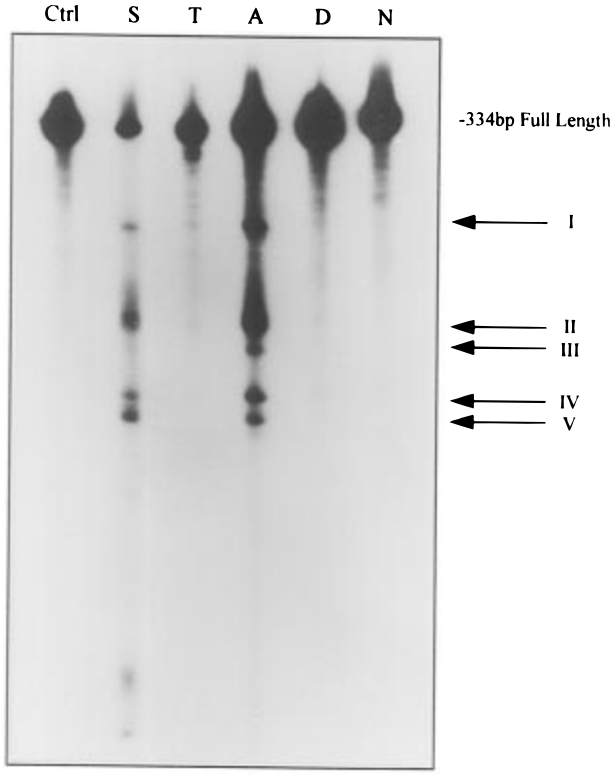

FIGURE 4: Autoradiogram illustrating the fragment patterns produced by the PBDs in the QIVT assay. A 2-μL aliquot from each experiment was electrophoresed on a 6% polyacrylamide gel and autoradiographed as described in Materials and Methods. The control (Ctrl) lane shows the full-length (334-base) RNA transcript produced as described. The remaining lanes show RNA fragments generated following incubation with sibiromycin (S), tomaymycin (T), anthramycin (A), DC-81 (D), or neothramycin (N). The positions of induced fragments I−V were established using the IVTF technique.

were used to calculate the percentage incorporation of radiolabeled rUTP.

In Vitro Transcription Footprinting (IVTF) Assay. The transcription (Tc) buffer described above was employed. A ternary complex was formed by incubating the linearized plasmid with T7 RNA polymerase (20 units) in the presence of 200 μM rGTP, 5 μM rATP, 5 μM rCTP, and [α-^{32}P]ATP for 10 min at 37 °C. Low concentrations of rNTPs were used to maximize incorporation of the radiolabel, thereby improving the sensitivity, and to optimize the production of a synchronized population of initiated complexes (i.e., minimize misincorporation and/or the effects of contaminating nucleotides). These conditions resulted in the production of a ternary complex with a nascent 14-mer RNA due to exclusive initiation at the +1 position. Heparin was added to a final concentration of 400 μg/mL to remove any nonspecifically bound RNA polymerase, and the mixture was incubated for 5 min at 37 °C. The PBD was then added at different PBD:DNA concentration ratios, and the mixture was incubated for 1 h in order to observe any concentration-dependent response. Following equilibration with the PBD, a nucleotide mix containing all ribonucleotides was added to achieve a final concentration of 2.0 mM for all ribonucleotides, and incubation was continued for 15 min at 37 °C. The elongation reaction was stopped by the addition of an equal volume of loading/blockage buffer comprising 90%

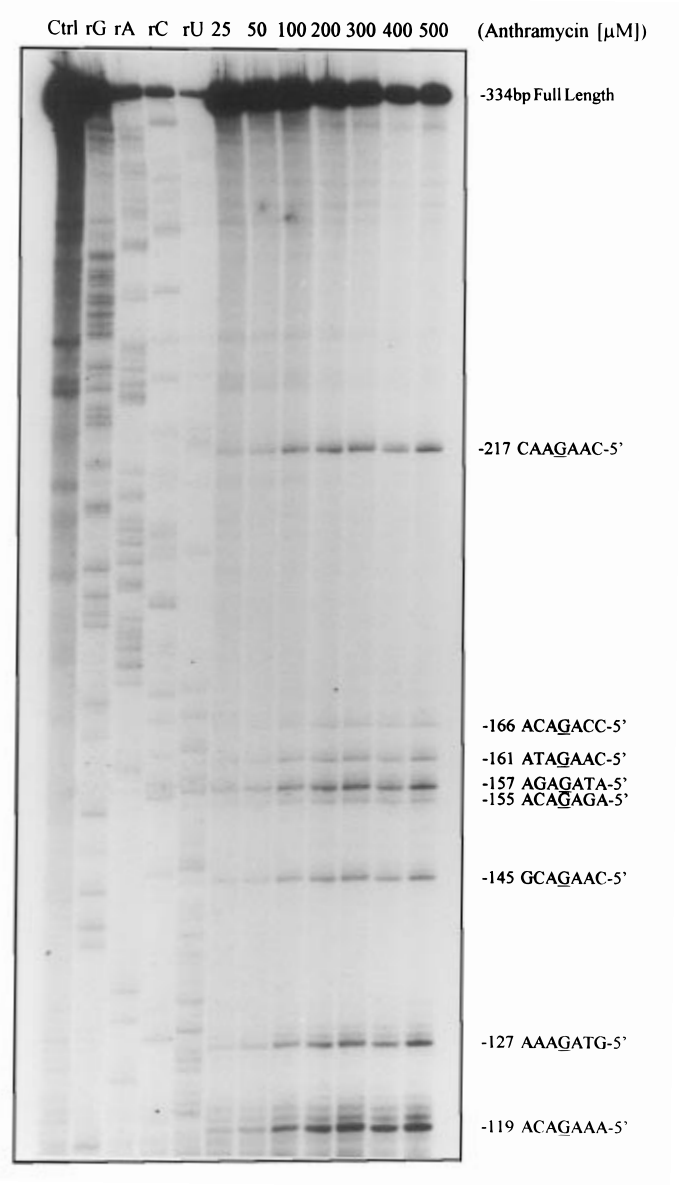

FIGURE 5: Concentration dependence for *in vitro* transcription blockage by anthramycin. Transcription initiation, DNA−PBD adduct formation, and elongation were carried out as described in Materials and Methods. The control (Ctrl) lane represents the full-length transcript following elongation in the absence of added PBD. Lanes rG, rA, rC, and rU are sequencing lanes generated for the appropriate ribonucleotides. The remaining lanes represent increasing concentrations of anthramycin (25−500 μM). The lengths and corresponding sequences (with the modified guanine underlined) for the major blockage sites are indicated.

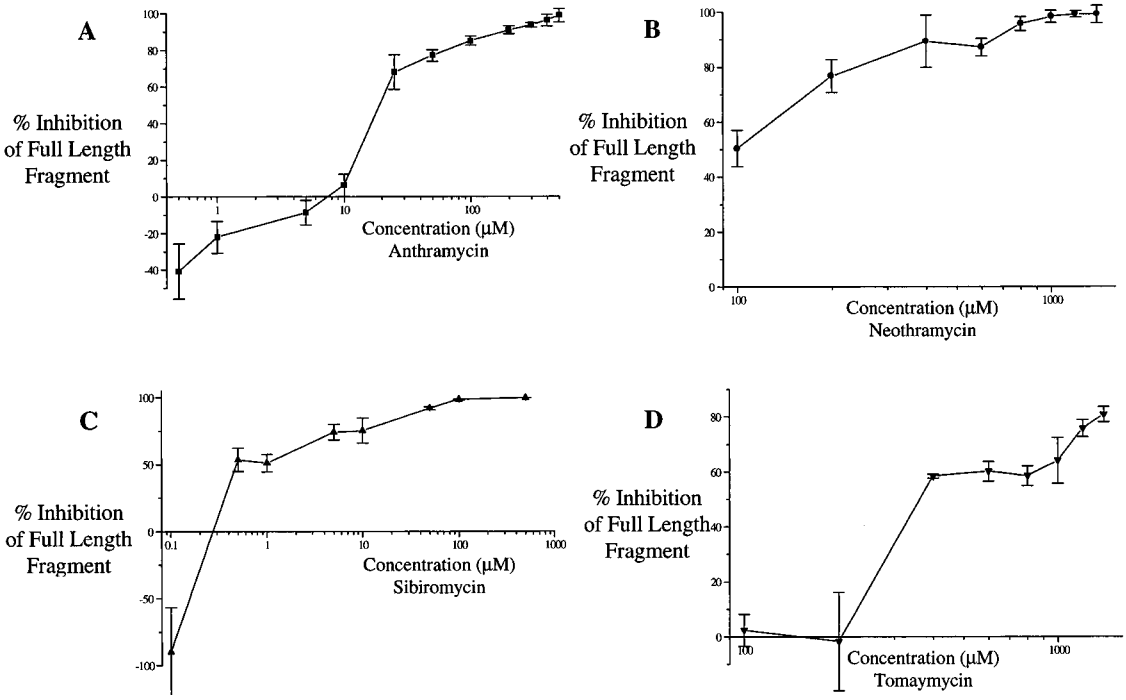

FIGURE 6: Inhibition of *in vitro* transcription by (A) anthramycin, (B) neothramycin, (C) sibiromycin, and (D) tomaymycin. The relative inhibition is based on the amount of full-length RNA fragment present due to PBD binding to the DNA template compared to that present in the drug-free control reaction.

formamide, 50 mM EDTA, 0.1% xylene cyanol, and 0.1% bromophenol blue.

RNA Sequencing. The method employed used 3′-deoxyribonucleotides of GTP, ATP, CTP, and UTP. Sequence information was obtained by adding one of four elongation nucleotide mixes, each containing the appropriate 3′-drNTP (300 μM) and rNTP (1 mM), where N is G, A, C, or U. The elongation reactions were continued for 10 min at 37 °C and stopped by the addition of the loading/blockage buffer.

MPE−Fe(II) Footprinting Analysis. The pGEM-2-N-*ras* plasmid was 5′-singly end-radiolabeled and purified using published procedures (Maniatis, 1989). A series of PBD concentrations were then incubated with the DNA for 1 h at 37 °C. The concentration used for each PBD was approximately equivalent to the concentration determined to inhibit *in vitro* transcription by 50%. Solutions were added to give final concentrations of 5 μM MPE, 4 μM Fe(II), and 2 mM DTT in each reaction mix. The mixtures were allowed to react at room temperature for 6 min, and then the reactions were stopped by cooling in a dry ice/ethanol bath for 5 min. Each frozen reaction mix was then lyophilized, and the resulting pellets washed with 0.3 M NaOAc and precipitated with ethanol. Loading/blockage buffer was added to all drug-treated and sequence marker samples prior to gel electrophoresis.

Sequence Marker Depurination. An aliquot of the 5′-end-labeled DNA (1 μg) was treated with 75% formic acid for 7 min at room temperature, which resulted in depurination of the DNA. An equal volume of "stop mix" containing 0.6 M NaOAc, 20 mM Na_2EDTA, tRNA (100 μg/mL), and ethanol 95% was added, and the mixture was chilled and centrifuged prior to supernatant removal. The pellet was lyophilized and digested in 10% aqueous piperidine solution, heated for 30 min at 90 °C, and then lyophilized after snap freezing. The resulting pellet was washed with water and then re-lyophilized prior to gel loading. RNA fragment analysis was performed using a Molecular Dynamics model 400B PhosphoImager, with quantitation using the supplied ImageQuant software.

Gel Electrophoresis of RNA and DNA Fragments. Samples from both the IVTF and MPE−Fe(II) footprinting experiments were heated for 5 min at 90 °C and then cooled in ice. Samples (5 μL) were loaded onto a 0.35 mm × 80 cm denaturing (6−8%) polyacrylamide gel in TBE buffer. Gels were pre-electrophoresed for 1 h at 3000 V to raise the temperature of the gel to ∼60 °C and to ensure denaturing conditions. Electrophoresis was continued until the xylene cyanol marker migrated approximately two-thirds down the gel length. Following electrophoresis, gels were dried at 80 °C onto one layer of Whatman 3MM and one layer of DE81 filter papers on a Bio-Rad model 583 gel dryer connected to a vacuum. Autoradiography was performed with Hyperfilm MP (Amersham) for 12 h at −70 °C without an intensifying screen for sharper images.

RESULTS

QIVT Assay. The percentage incorporation of radiolabeled rUTP was calculated in order to determine the rank order for inhibition of *in vitro* transcription by the PBDs examined in this study. The data presented in Figure 3 show a sibiromycin > tomaymycin > anthramycin > DC-81 > neothramycin ranking order for inhibition at a PBD concentration of 100 μM. Interestingly, stimulation of transcription was evident for sibiromycin and neothramycin at low doses of added compound (data not shown). An autoradiogram of the transcription experiments (Figure 4) reveals that both sibiromycin and anthramycin induce premature termination of transcription that results in the formation of shorter RNA fragments.

IVTF Assay. An autoradiogram produced from the IVTF assay with anthramycin is shown in Figure 5. Using phosphoimage analysis, the full-length and short fragments

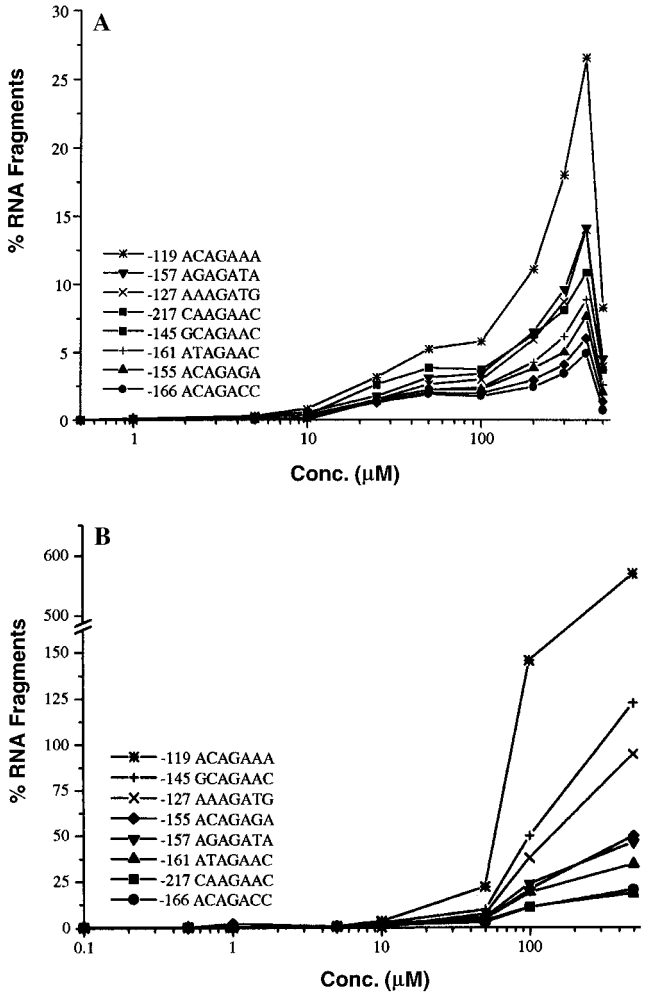

FIGURE 7: Percentage of RNA fragments present relative to the full-length fragment in the IVTF experiments for (A) anthramycin and (B) sibiromycin at different concentrations..

observed on each gel were quantitated. From these data, a concentration-dependent response was found, and a rank order for inhibition of transcription was determined as: sibiromycin > anthramycin > neothramycin > tomaymycin (Figure 6). Interestingly, stimulation of transcription was seen at low concentrations of sibiromycin and anthramycin, as also indicated from the QIVT experiments. Tomaymycin also showed some evidence of stimulation at low concentrations, although to a much lesser extent.

Figure 5 reveals that this DNA sequence has discrete binding sites for anthramycin that cause blockage of transcription. Using the sequence lanes (rG, rA, rC, and rU), it can be established that the blockage sites correspond exclusively to AG̲A-5′ sequences. Furthermore, there is a preferred order of blockage-site sequences for both anthramycin and sibiromycin which evidently relates to the sequences of flanking base pairs. Phosphoimaging analysis for anthramycin indicates a preferred order for ACAG̲AAA-5′ (119-mer) > AGAG̲ATA-5′ (157-mer) > AAAG̲ATG-5′ (127-mer) > CAAG̲AAC-5′ (217-mer) > GCAG̲AAC-5′ (145-mer) > ATAG̲AAC-5′ (161-mer) > ACAG̲AGA-5′ (155-mer) > ACAG̲ACC-5′ (166-mer) sequences, where the indicated guanine base is alkylated (Figure 7A). In contrast, the preferred order for site blockage by sibiromycin is given by ACAG̲AAA-5′ (119-mer) > GCAG̲AAC-5′ (145-mer) > AAAG̲ATG-5′ (127-mer) > ACAG̲AGA-5′ (155-mer) > AGAG̲ATA-5′ (157-mer) > ATAG̲AAC-5′ (161-mer) > CAAG̲AAC-5′ (217-mer) = ACAG̲ACC-5′ (166-mer) (Figure 7B).

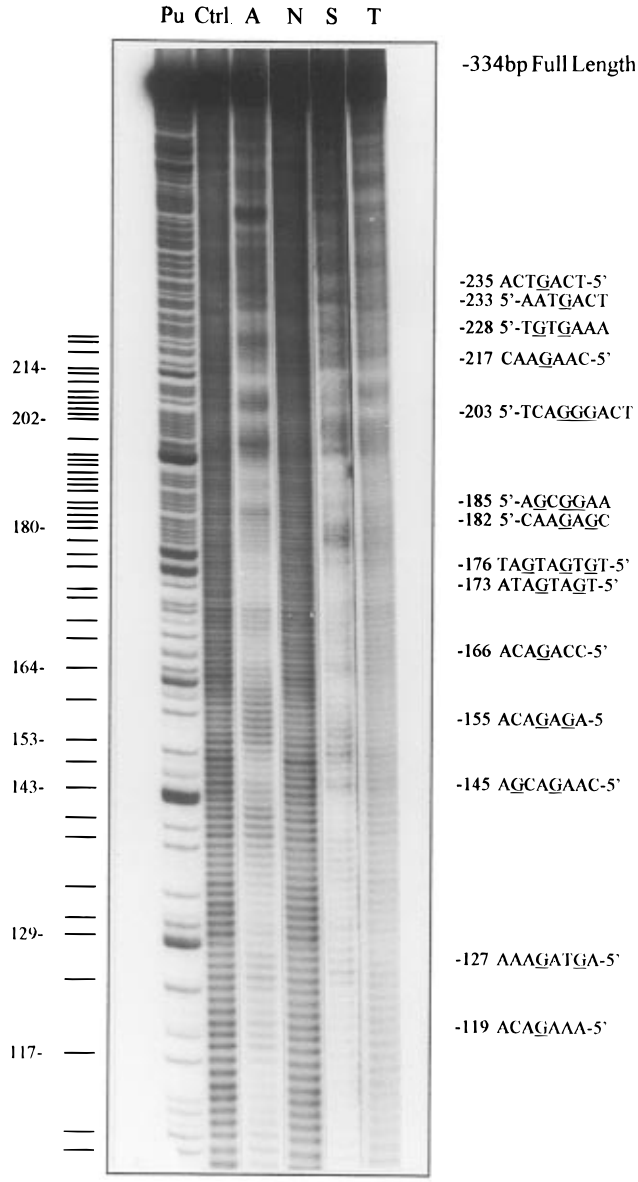

FIGURE 8: Autoradiogram for DNA binding by the PBDs determined using MPE−Fe(II) footprinting. The left-hand lane (Pu) is a purine sequence marker lane involving formic acid and piperidine treatment as described. The corresponding base numbers are indicated on the left-hand side. Lanes: (Ctrl) MPE−Fe(II)-treated DNA in the absence of a PBD; (A) 20 μM anthramycin; (N) 100 μM neothramycin; (S) 1 μM sibiromycin; and (T) 300 μM tomaymycin. Each PBD was incubated with the 5′-end-labeled pGEM-2-N-*ras* for 1 h. The estimated positions and sequences (with the covalently-modified guanines underlined) of the major binding sites are indicated on the right-hand side.

Tomaymycin and neothramycin produced blockages at the equivalent sites (data not shown), but showed no particular order of preference for these sequences. However, additional blockage sites were observed at AG̲G-5′ (293), GG̲A-5′ (302), and TG̲A-5′ (194 and 208) for both compounds.

MPE−Fe(II) Footprinting. Figure 8 shows an MPE−Fe(II) footprinting autoradiogram obtained for the four PBDs examined, at drug concentrations equivalent to those required to cause 50% inhibition of transcription in the IVTF study and with the same incubation period (1 h). As expected from the IVTF results, neothramycin and tomaymycin did not

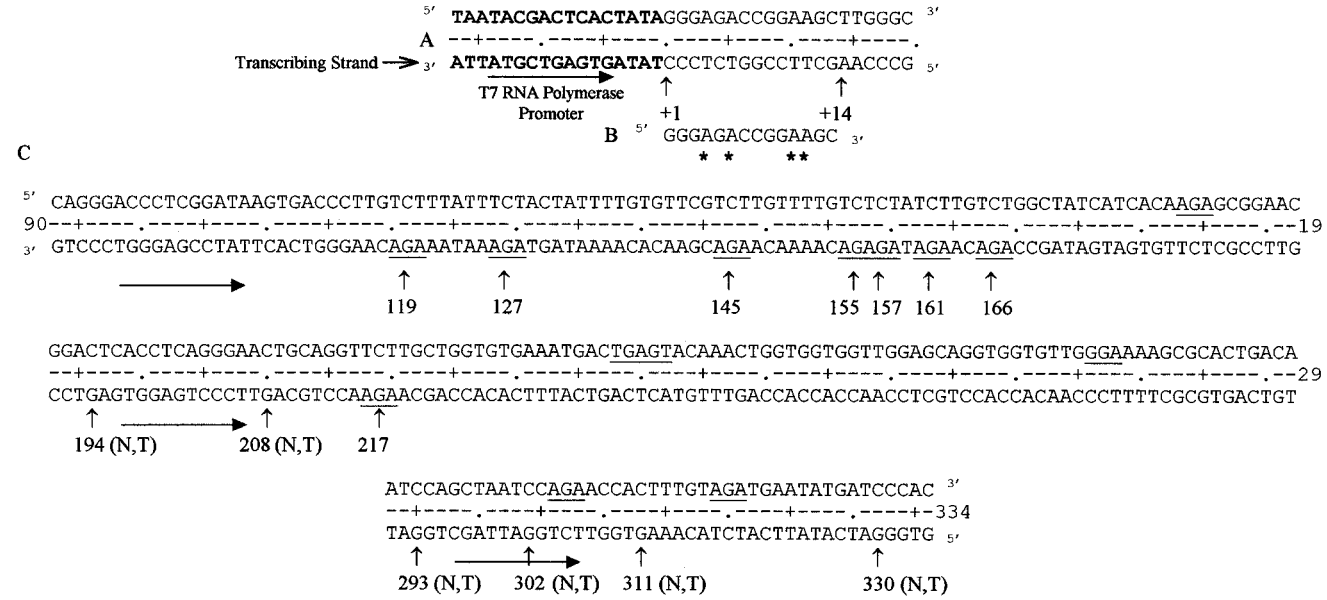

FIGURE 9: Sequence analysis for DNA−PBD adducts leading to transcription blockage. (A) Sequence of the T7 RNA polymerase promoter region showing the lower 3′−5′ transcribing strand and the upper, nontemplate 5′−3′ strand. (B) Sequence of the 14-mer mRNA fragment present in the ternary complex (***** indicates the rATP radiolabel incorporated during formation of the ternary complex). The horizontal arrow indicates the direction of transcription. (C) Transcribing N-*ras* fragment (bases 90−334). The vertical arrows correspond to the positions at which transcription is blocked by covalent DNA adducts with the PBDs examined. Those positions due exclusively to neothramycin and tomaymycin adducts are indicated by (N,T). Optimal 5′-A**G**A sequences on each strand are underlined.

produce pronounced footprints under these conditions. However, both anthramycin and sibiromycin gave strong footprints corresponding to binding sites on both the transcribed and nontranscribed DNA strands. Interestingly, the preferred binding sites (e.g., −173, −176, −182, and −185) did not correlate with those transcription blocks observed in the IVTF study whereas, conversely, certain sequence sites that caused T7 RNA polymerase blocks (e.g., −119, −155, −157, and −161) did not appear as significantly strong MPE−Fe(II) footprints. The majority of DNA−PBD adducts revealed by the MPE−Fe(II) footprinting assay represent 5′-Pu-**G**-Pu target sequences and (to a lesser extent) 5′-Pu-**G**-Py and 5′-Py-**G**-Pu sequences (e.g., −173, −176, and −233), whereas transcription inhibition appears to be due mainly to 5′-AGA sequences.

DISCUSSION

The rank order of potency for the inhibition of *in vitro* transcription determined from the QIVT assay is similar to that established by unrelated studies of covalent DNA reactivity (Puvvada et al., 1993), other than an apparent reversal of activity for anthramycin and tomaymycin. Thus, by QIVT, sibiromycin is the most potent PBD inhibitor, followed by tomaymycin and anthramycin, with both DC-81 and neothramycin providing markedly poorer inhibition. From the QIVT experiments (Figure 4), it is clear that formation of a DNA−PBD adduct can interfere with the linear diffusion of a DNA-processing enzyme (as indicated by shorter RNA fragments) and seriously hamper the recognition capacity for key DNA sequences (as indicated by a reduction in full-length RNA fragments) (Balcarova et al., 1992).

The QIVT assays indicate that tomaymycin is a more potent inhibitor of *in vitro* transcription than either anthramycin or neothramycin, whereas the IVTF data (e.g., Figure 6) suggest that tomaymycin has the weakest activity. One possible explanation for this observation may relate to covalent binding of tomaymycin in the promoter region, resulting in interference with recognition by the promoter T7 polymerase and/or inhibition of formation of the initiation complex. Although neothramycin and DC-81 also showed evidence of inhibiting *in vitro* transcription, they did not show significant formation of fragments. This behavior suggests that, as with tomaymycin, these PBD agents may bind predominantly to the promoter region of the DNA template, thereby inhibiting the T7 initiation process.

Molecular modeling studies using the same sequence of pGEM-2-N-*ras* (to be reported elsewhere) suggest that AGA-5′ represents the most energetically-preferred sequence for adduct formation with the PBDs used. The IVTF data therefore suggest that the T7 RNA polymerase may stop transcribing at the most energetically-preferred PBD binding sites on the duplex, whereas it can "read through" less-energetically-favorable adducts. This phenomenon has also been observed for established DNA intercalants, including nogalamycin, actinomycin D, and adriamycin (White & Phillips, 1989a−c). Interestingly, reported studies with intercalators and bacterial *E. coli* RNA polymerase show the same transcribing characteristics, suggesting that the catalytic site and melted region of the RNA−DNA hybrid in the ternary complex are virtually coincident for both types of polymerase (Shi et al., 1987; White & Phillips, 1988). Selective initiation of the T7 promoter from the +1 position results in RNA from the initiated complex that is 14 bases long (Figure 9). Comparative studies of the effect of intercalators on *in vitro* transcription have shown that T7 polymerase is far less stable than *E. coli* RNA polymerase when the elongation complex is paused at a DNA−drug adduct (White & Phillips, 1989a−c). Furthermore, the bacterial RNA polymerase revealed an ability to "read through" past the drug site, whereas the phage RNA polymerase resulted only in the termination of transcription. This stability difference has been confirmed from observations that *E. coli* transcription complexes survive nondena-

turing PAGE (Straney & Crothers, 1985), whereas T7 complexes dissociate under similar conditions (Shi et al., 1987). This would suggest that the presence of a covalent DNA−PBD adduct on the transcribing strand may be sufficient to destabilize the T7 ternary complex, possibly due to (i) localized DNA conformational changes and/or accumulated steric effects, and/or (ii) as a direct consequence of drug-induced arrest of the elongation complex. On the basis of comparing T7 polymerase with *E. coli* polymerase, PBD-induced blockage of transcription in the IVTF studies may be due to termination of the elongation process as opposed to pausing, although an investigation of the effects of elongation time would be required to confirm this suggestion. Inhibition of transcription, however, may occur by more than one pathway (e.g., inhibition of protein binding and/or inhibition of elongation), and the results reported here cannot distinguish between different modes of inhibition, but instead represent an average of what must be occurring in solution. Future experiments will seek to determine the precise mode of inhibition for each compound.

Finally, the observed stimulation of transcription at low concentrations of sibiromycin and neothramycin suggests that the highest affinity sites (i.e., those sites that are most likely to be "hit" at low PBD concentrations) actually stimulate rather than inhibit transcription. We have no explanation for this phenomenon at present, although it will be the subject of future investigations.

In conclusion, the QIVT and IVTF studies described here clearly demonstrate, for the first time, PBD-induced disruption of transcription. The possible importance of PBD binding sites in the promoter region has also been established. It appears that although the DNA-binding affinities of the PBDs (as measured by assays such as the RED_{100} and also molecular modeling studies) contribute to the inhibition of transcription, the binding sequence involved and structural characteristics of the DNA−PBD adducts may also play a major role in determining the effectiveness of drug-induced blockage. The difference between the DNA−PBD adducts revealed by the MPE−Fe(II) footprinting assay (majority represented by 5′-Pu-**G**-Pu and, to a lesser extent, 5′-Pu-**G**-Py and 5′-Py-**G**-Pu) and transcription inhibition (predominantly 5′-AGA sequences) can be explained by the T7 polymerase halting only at the most stable covalently-bound PBD−DNA adducts. It is conceivable that MPE−Fe(II) footprinting may also detect noncovalently bound PBD−DNA adducts for which there is some evidence of existence (Thurston, 1993). The observed stimulation of transcription by sibiromycin and neothramycin at low concentrations is intriguing and will be the subject of future studies. Although it is not possible to establish the precise mechanism of either the inhibition or stimulation of transcription from the results reported here, future studies involving kinetic experiments and the use of DNA containing a known number of PBD binding sites at defined sequences should address these issues.

REFERENCES

Balcarova, Z., Mrazek, J., Kleinwachter V., & Brabec, V. (1992) *Gen. Physiol. Biophys. 11*, 579−588.

Bose, D. S., & Thurston, D. E. (1993) *Tetrahedron Lett. 34*, 1377−1378.

Bose, D. S., Jones, G. B., & Thurston, D. E. (1992) *Tetrahedron 48*, 751−758.

Cullinane, C., Cutts, S. M., Rosmalen, A. V., & Phillips, D. R. (1994) *Nucleic Acids Res. 22*, 2296−2303.

Gray, P. J., Cullinane, C., & Phillips, D. R. (1991) *Biochemistry 30*, 8036−8040.

Hertzberg, R. P., Hecht, S. M., Reynolds, V. L., Molineux, I. J., & Hurley, L. H. (1986) *Biochemistry 25*, 1249−1258.

Hurley, L. H., Gairola, C., & Zmijewski, M. (1977) *Biochim. Biophys. Acta 475*, 521−535.

Hurley, L. H., Reck, T., Thurston, D. E., Langley, D. R., Holden, K. G., Hertzberg, R. P., Hoover, J. R. E., Gallagher, G., Faucette, L. F., Mong, S. M., & Johnson, R. K. (1988) *Chem. Res. Toxicol. 1*, 258−268.

Kopka, M. L., Goodsell, D. S., Baikalov, I., Grzeskowiak, K., Cascio, D., & Dickerson, R. E. (1994) *Biochemistry 33*, 13593−13610.

MacDonald, L. E., Zhou, Y., & McAllister, W. T. (1993) *J. Mol. Biol. 232*, 1030−1047.

Maniatis, T., Fritsch, E. F., & Sambrook, J. (1989) in *Molecular Cloning: A Laboratory Manual*, 2nd ed., Cold Spring Harbor Laboratory Press, Cold Spring Harbor, New York.

Masta, A., Gray, P. J., & Phillips, D. R. (1994) *Nucleic Acids Res. 22*, 3880−3886.

Panousis, C., & Phillips, D. R. (1994) *Nucleic Acids Res. 22*, 1342−1345.

Phillips, D. R., & Crothers, D. M. (1986) *Biochemistry 25*, 7355−7362.

Phillips, D. R., White, R. J., & Cullinane, C. (1989) *FEBS Lett. 246*, 233−240.

Phillips, D. R., Cullinane, C., Trist, H., & White, R. J. (1990a) *In vitro* transcription analysis of the sequence specificity of reversible and irreversible complexes of adriamycin with DNA. In *The Jerusalem Symposia on Quantum Chemistry and Biochemistry* (Pullman, B., & Jorter, J., Eds.) Vol. 23, pp 137−155, Kluwer, Jerusalem.

Phillips, D. R., White, R. J., Dean, D., & Crothers, D. M. (1990b) *Biochemistry 29*, 4812−4819.

Phillips, D. R., White, R. J., Trist, H., Cullinane, C., Dean, D., & Crothers, D. M. (1990c) *Anti-Cancer Drug Des. 5*, 21−29.

Phillips, D. R., Moate, P. J., & Boston, R. C. (1994) *Anti-Cancer Drug Des. 9*, 209−219.

Pierce, J. R., Nazimiec, M., & Tang, M. (1993) *Biochemistry 32*, 7069−7078.

Puvvada, M. S., Hartley, J. A., Jenkins, T. C., & Thurston, D. E. (1993) *Nucleic Acids Res. 21*, 3671−3675.

Remers, W. (1988) in *The Chemistry of Antitumor Antibiotics*, Vol. 2, pp 28−92, Wiley & Son, New York.

Shi, Y., Gamber, H., & Hearst, J. (1987) *J. Biochem. 263*, 527−534.

Skorobogaty, A., White, R. J., Phillips, D. R., & Reiss, J. A. (1988) *Drug Des. Delivery 3*, 125−152.

Straney, D. C., & Crothers, D. M. (1985) *Cell 43*, 449−459.

Thurston, D. E. (1993) in *Molecular Aspects of Anticancer Drug−DNA Interactions* (Neidle, S., & Waring, M. J., Eds.) Vol. 1, pp 54−88, Macmillan Press, U.K.

Trist, H., & Phillips, D. R. (1989) *Nucleic Acids Res. 17*, 3673−3688.

White, R. J., & Phillips, D. R. (1988) *Biochemistry 27*, 9122−9132.

White, R. J., & Phillips, D. R. (1989a) *Biochem. Pharmacol. 38*, 331−334.

White, R. J., & Phillips, D. R. (1989b) *Biochemistry 28*, 4277−4283.

White, R. J., & Phillips, D. R. (1989c) *Biochemistry 28*, 6259−6269.

BI952490R